Numerical analysis of fluid flow in a three-dimensional porous enclosure by the Boundary Element Method

J. Kramer Stajnko[1], R. Jecl[1], J. Ravnik[2] & L. Škerget[2]
[1]*Faculty of Civil Engineering, University of Maribor, Slovenia*
[2]*Faculty of Mechanical Engineering, University of Maribor, Slovenia*

Abstract

In the present paper a three-dimensional numerical code for simulation of porous media flow is presented which is based on the Boundary Element Method (BEM). The most general mathematical model is used to describe momentum, energy and solute transport in porous media which are based upon the general Navier–Stokes equations valid for the pure fluid flow. The developed numerical algorithm enables detailed investigation of the fluid flow together with heat and solute transfer under various conditions given with different governing parameters, e.g. thermal and solutal Rayleigh numbers, Darcy number, Lewis number, buoyancy coefficient. In the paper the effect of different governing parameters on the rate of heat, solute and momentum transfer are investigated. Under a certain range of parameters, complex flow patterns occur which exhibits the importance for us to investigate the problem in three dimensions.
Keywords: porous medium flow, simultaneous heat and solute transport, Boundary Element Method, Brinkman-extended Darcy formulation.

1 Introduction

Transport phenomenon in porous media is characterized with complex interactions between solid matrix and a moving fluid and has been motivated by a broad range of engineering applications including environmental, industrial, agricultural applications, e.g. contaminant transport through water saturated soils, ground water pollution, water movement in geothermal reservoirs. Diverse engineering

WIT Transactions on The Built Environment, Vol 129, © 2013 WIT Press
www.witpress.com, ISSN 1743-3509 (on-line)
doi:10.2495/FSI130081

applications have motivated scientific community to find efficient models and approaches to simulate fluid flow and transport processes in porous media.

Different analytical, numerical, as well as experimental studies can be found in the literature where simultaneous heat and solute transfer in porous media is simulated. Mainly, there are two configurations on which the convective flow have been studied. The first example is horizontal porous layer which is subjected to vertical temperature and concentration gradients where primarily the critical conditions for the onset of convective motion on the basis of linear stability analysis are considered and can be found in [1–3]. The second possible configuration is a vertical cavity filled with porous media where the vertical walls are maintained at different values of temperature and concentration. For this configuration two types of examples are possible; the resulting thermal and concentration buoyancy forces can aid or oppose each other. There are several published studies considering both examples, e.g. [4–7].

Only a few studies exist which consider three-dimensional analysis of fluid flow and simultaneous heat and solute transfer in porous enclosure. First study of this kind, where the problem of double-diffusive natural convection in porous cavity due to opposing buoyancy forces was considered, was published by Sezai and Mohamad [8]. Their results reveal that for the certain parameter ranges the flow structure becomes three-dimensional with second flow formation that can not be captured with two-dimensional models. In addition, Mohamad *et al.* [9] published three-dimensional study of the problem where the effect of lateral aspect ratio is studied.

In the present paper a problem of double-diffusive natural convection in porous media for three-dimensional geometry is studied using the BEM solver. At the beginning the general mathematical model based on the macroscopic Navier–Stokes equations is given. In addition, the numerical method is briefly outlined. The obtained numerical results are validated with comparison with other numerical results available in the literature. Furthermore, the influence of some governing parameters on the convective motion in porous enclosure are analyzed, focusing on the situations where the flow may become three-dimensional.

2 Mathematical model

The present work refers to a problem of double-diffusive natural convection in a three-dimensional cavity, fully filled with fluid saturated porous medium. The mathematical model is based on the conservation laws for mass, momentum, energy and species concentration which primarily describe the pure fluid flow and are written at the microscopic level, in general. Since the geometry of porous media is irregular and complex, the conventional fluid mechanics can not be used to describe what happens in every point of the fluid-solid matrix. In order to describe fluid flow in porous media on a global level and to simplify the mathematical description, all flow quantities of interest are volume-averaged which is amenable to theoretical treatment. The laws governing the macroscopic variables are derived from the standard equations obeyed by the fluid by spatial approach where the

macroscopic variable is defined as an appropriate mean over a sufficiently large representative elementary volume (REV). The length scale of the REV has to be much larger than the pore scale and considerably smaller than the length scale of the macroscopic flow domain. The detailed averaging procedure for all governing equations is given in [10]. The macroscopic governing equations in non-dimensional form can be written as:

$$\vec{\nabla} \cdot \vec{v} = 0, \tag{1}$$

$$\frac{1}{\phi}\frac{\partial \vec{v}}{\partial t} + \frac{1}{\phi^2}(\vec{v}\cdot\vec{\nabla})\vec{v} = -Ra_T\ Pr(T + N\ C)\vec{g} - \frac{1}{Eu}\vec{\nabla}p + \frac{1}{\phi}Pr\nabla^2\vec{v} - \frac{Pr}{Da}\vec{v}, \tag{2}$$

$$\sigma\frac{\partial T}{\partial t} + (\vec{v}\cdot\vec{\nabla})T = \frac{\lambda_e}{\lambda_f}\nabla^2 T, \tag{3}$$

$$\phi\frac{\partial C}{\partial t} + (\vec{v}\cdot\vec{\nabla})C = \frac{1}{Le}\nabla^2 C, \tag{4}$$

where the following volume averaged and dimensionless variables for velocity, position vector, time, temperature, concentration and gravitational acceleration are used respectively:

$$\vec{v} \to \frac{\vec{v}}{v_0},\ \vec{r} \to \frac{\vec{r}}{L},\ t \to \frac{v_0 t}{L}, T \to \frac{T - T_0}{\Delta T},\ C \to \frac{C - C_0}{\Delta C},\ \vec{g} \to \frac{\vec{g}}{g_0}. \tag{5}$$

v_0 is characteristic velocity and is given as $v_0 = \lambda_f/(\rho c_p)_f L$, where λ_f is fluid thermal conductivity, $(\rho c_p)_f$ is fluid heat capacity, ρ is density, c_p is specific heat at constant pressure and L characteristic length. This formulation for characteristic velocity is common for buoyant flow simulations. Furthermore, T_0 and C_0 are characteristic temperature and concentration, ΔT and ΔC characteristic temperature and concentration differences, while $g_0 = 9.81 m/s^2$. Further parameters in governing equations (1)-(4) are: ϕ porosity, p pressure, σ heat capacity ratio $\sigma = (\phi\ c_f + (1-\phi)c_s)/c_f$, where $c_f = (\rho c_p)_f$ and $c_s = (\rho c_p)_s$ are heat capacities for fluid and solid phases respectively, λ_e is the effective thermal conductivity of the fluid saturated porous media given as $\lambda_e = \phi\lambda_f + (1-\phi)\lambda_s$, where λ_f and λ_s are thermal conductivities for fluid and solid phases respectively. Moreover, following non-dimensional numbers are used:

- Ra_T, thermal fluid Rayleigh number $Ra_T = g\beta_T \Delta T L^3/\nu\alpha$, where β_T is volumetric thermal expansion coefficient, ν is kinematic viscosity and α is thermal diffusivity given as $\alpha = \lambda_f/c_f$,
- Pr, Prandtl number $Pr = \nu/\alpha$,
- N, buoyancy coefficient $N = Ra_S/Ra_T$, where Ra_S is solutal Rayleigh number $Ra_S = g\beta_C \Delta C L^3/\nu\alpha$, where β_C is volumetric expansion coefficient due to chemical species,
- Eu, Euler number $Eu = \rho v^2/p$,
- Da, Darcy number $Da = K/L^2$, where K is permeability of porous media,
- Le, Lewis number $Le = \alpha/D$, where D is mass diffusivity.

The momentum equation (2) is coupled with energy (3) and species equation (4) due to the buoyancy term, which is described with the Oberbeck Boussinesq approximation, considering the fact that the fluid density depends only on temperature and concentration variations:

$$\rho = \rho_0(1 - \beta_T(T - T_0) - \beta_C(C - C_0)). \tag{6}$$

The momentum equation (2) is also known as the Darcy-Brinkman equation, with two viscous terms e.g. Brinkman viscous term (third on the r.h.s) and Darcy viscous term (fourth on the r.h.s.). The Brinkman viscous term is analogous to the Laplacian term in the classical Navier–Stokes equations for pure fluid flow. It expresses the viscous resistance or viscous drag force exerted by the solid phase on the flowing fluid at their contact surfaces. With the Brinkman term the non-slip boundary condition on a surface which bounds porous media is satisfied, as reported in [11].

2.1 Velocity-vorticity formulation

Introducing the velocity-vorticity formulation to the governing set of equations the computational scheme is partitioned into kinematic and kinetic computational part. The kinematics is governed with the velocity equation which is obtained from the mass conservation law (1). It is a vector elliptic partial differential equation of Poisson type and links the velocity and vorticity fields for every point in space and time and can be stated as [12]:

$$\nabla^2\vec{v} + \vec{\nabla} \times \vec{\omega} = 0, \tag{7}$$

where $\vec{\omega}$ is vorticity vector, defined as the curl of velocity field $\vec{\omega} = \vec{\nabla} \times \vec{v}$. The kinetics is governed by the vorticity transport equation, which is derived by taking the curl of the momentum equation (2), which reads as:

$$\begin{aligned} &\phi\frac{\partial\vec{\omega}}{\partial t} + (\vec{v}\cdot\vec{\nabla})\vec{\omega} = (\vec{\omega}\cdot\vec{\nabla})\vec{v} - PrRa_T\phi^2\vec{\nabla}\times(T + N\,C)\vec{g} + \\ &Pr\phi\nabla^2\vec{\omega} - \frac{Pr}{Da}\phi^2\vec{\omega}. \end{aligned} \tag{8}$$

The left hand side of equation (8) represents the advective vorticity transport and the terms on the right hand side are the vortex twisting and stretching term, the buoyancy term, the diffusion term and the Darcy term. The partial differential equations (7), (8), (3) and (4) represent the nonlinear system of equations for the unknown velocity, vorticity temperature and concentration fields.

3 Numerical method

For the solution of the governing equations a combination of single-domain and sub-domain BEM will be applied. All governing equations are written in an

integral form which is obtained by using the Green's second identity for the unknown field function and for fundamental solution $u^\star$ of the Laplace equation: $u^\star = 1/4\pi|\vec{\xi} - \vec{r}|$. The integral form of all governing equations is given in [12].

The system of equations is solved according to known Dirichlet or Neumann type boundary conditions for velocity, temperature and concentration. The no-slip boundary condition on all solid walls are used and the values of temperature and concentration or their fluxes are prescribed. Domain velocity values are calculated from kinematics equation (7), domain temperature values from energy equation (3) and domain concentration values from species equation (4). The boundary conditions of vorticity values, which are needed to solve the vorticity transport equation are unknown at the beginning and are calculated as a part of the algorithm. The numerical algorithm contains following steps:

1. Porous media properties are determined.
2. Vorticity values on the boundary are calculated by single-domain BEM from the kinematics equation (7).
3. Velocity values within the domain are calculated by sub-domain BEM from the kinematics equation (7).
4. Temperature values within the domain are calculated by sub-domain BEM from energy equation (3).
5. Concentration values within the domain are calculated by sub-domain BEM from the concentration equation (4).
6. Vorticity values within the domain are calculated by sub-domain BEM from the vorticity equation (8).
7. Check convergence. All steps from 2. until 6. are repeated until all flow fields achieve the required accuracy.

The numerical algorithm for simulation of three-dimensional fluid flow and heat transfer by a combination of single- and sub-domain BEM, was developed by [13, 14] and was adopted for simulation of flow and heat transfer in porous media by [12]. The solver has been, furthermore, adopted for simulation of simultaneous heat and solute transfer in porous media.

4 Results and discussion

The developed numerical scheme is used to investigate the steady three-dimensional flow patterns and the resulting heat and solute transfer within a cubic enclosure where the opposite walls are maintained at different temperature and concentration values while the rest of the walls are adiabatic and impermeable as shown in Fig.(1). The temperature and concentration gradients which occur near the vertical walls induce density differences in the fluid and subsequently the appearance of thermal and solutal buoyancy forces, respectively.

The overall heat and solute transfer under different conditions were studied focusing on the influence of different values of Darcy number ($Da = 10^{-6} \ldots 10^{-1}$) and buoyancy coefficient ($N = 2 \ldots -2$) at fixed values of Ra_P and Le. The results are expressed in terms of average Nusselt and Sherwood

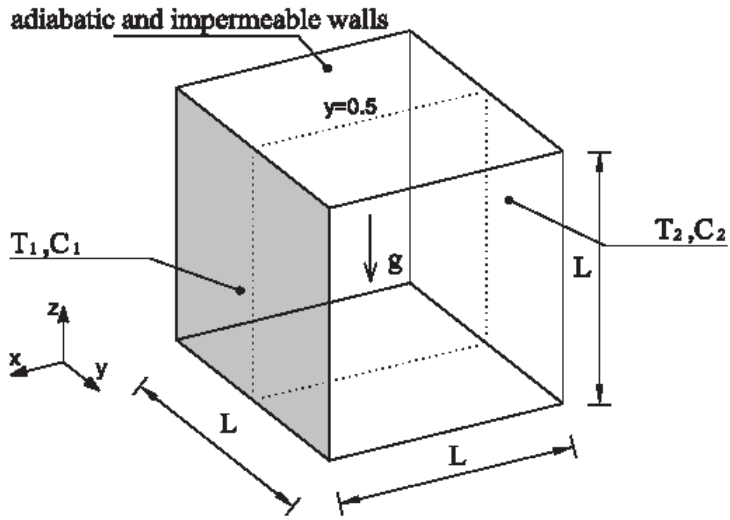

Figure 1: Geometry of the problem.

numbers which present the wall heat and species flux and are given as:

$$Nu = \int_{\Gamma} \vec{\nabla} T \cdot \vec{n} d\Gamma \, , \qquad Sh = \int_{\Gamma} \vec{\nabla} C \cdot \vec{n} d\Gamma. \tag{9}$$

All calculations were performed on a nonuniform mesh with $20 \times 8 \times 20$ subdomains and 28577 nodes. Subdomains are concentrated towards the hot and a cold walls. The convergence criteria for all field functions was 10^{-5}, under-relaxation of vorticity, temperature and concentration values ranging from 0.1 to 0.01 was used. The results for double-diffusive natural convection for different values of governing parameters are firstly compared with solutions from the study [9] and are presented in Tables 1 and 2. In this case the solutal and thermal buoyancy forces are opposing each other, which is given with $N < 0$. The value of Prandtl number is $Pr = 10$ and the porous medium properties are $\phi = 1$ and $\sigma = 1$. The numerical results in the reference study are obtained using the principle of finite volume method. From the results it may be seen that the agreement with reference solutions is good for all different values of governing parameters.

Due to boundary conditions considered in this study where the left-hand side wall is maintained at higher temperature and concentration values as the right-hand side wall, the resulting flow direction due to thermal buoyancy forces is clockwise, while the direction of the solutal buoyancy forces depends on the sign of the buoyancy coefficient. In case when $N < 0$, the direction of solutal flow is counterclockwise and is opposing the thermal flow.

Furthermore, the influence of Darcy number and buoyancy coefficient on overall heat and mass transfer in the cavity were investigated. The results of average

Table 1: Nusselt and Sherwood number values for 3D natural convection in a cubic enclosure for $Ra_P = 10$, $Da = 10^{-6}$, $N = -0.5$ and different values of Lewis number. The reference results are from the study of [9].

$Ra_P = 10$; $Da = 10^{-5}$; $N = -0.5$				
		$Le = 1$	$Le = 10$	$Le = 100$
Nu	Present	**1.019**	**1.039**	**1.048**
	Ref.	1.0198	1.0404	1.0424
Sh	Present	**1.019**	**2.450**	**4.743**
	Ref.	1.0198	2.4467	4.7511

Table 2: Nusselt and Sherwood number values for 3D natural convection in a cubic enclosure for $Ra_p = 1$, $Da = 10^{-6}$, $Le = 50$ and different values of buoyancy coefficient. The reference results are from the study of [9].

$Ra_P = 1$; $Da = 10^{-6}$; $Le = 50$			
		$N = -0.2$	$N = -0.5$
Nu	Present	**1.0005**	**1.0002**
	Ref.	1.0006	1.0003
Sh	Present	**1.9627**	**1.5524**
	Ref.	1.9517	1.5495

Nusselt and Sherwood number values at fixed values of porous Rayleigh number $Ra_P = 100$ and Lewis number $Le = 10$ and various Da and N are shown graphically in Figs 4 and 5. In case when $N = 0$ the only acting force is thermal buoyancy force. With any increase of N in positive direction, the Nusselt and Sherwood numbers increase at any value od Darcy number. On the other hand, both the Nusselt and Sherwood numbers decrease upon increasing the magnitude of N in the negative direction between $-0.5 > N > -1.5$ at any value of Darcy number. The opposing buoyancy effect due to solutal variations become dominant in this case which slow down the thermal buoyancy force. For $N = -1.0$, Nu value is close to the diffusive solution ($Nu \approx 1$) which is a result of equal intensity of thermal and solutal effects with opposing directions. With further increasing N

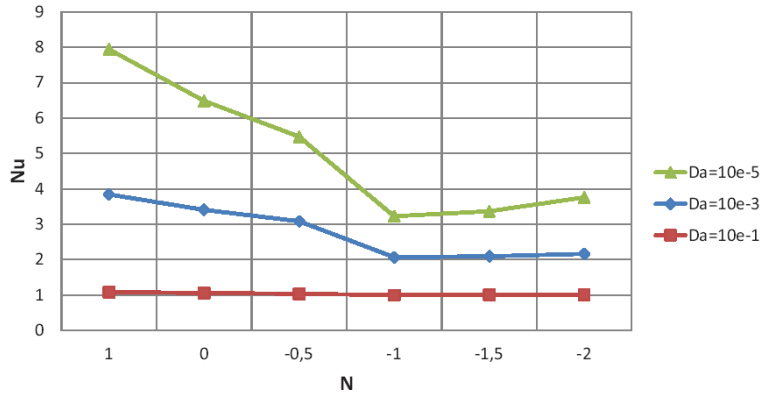

Figure 2: Nusselt number values for different Da and N.

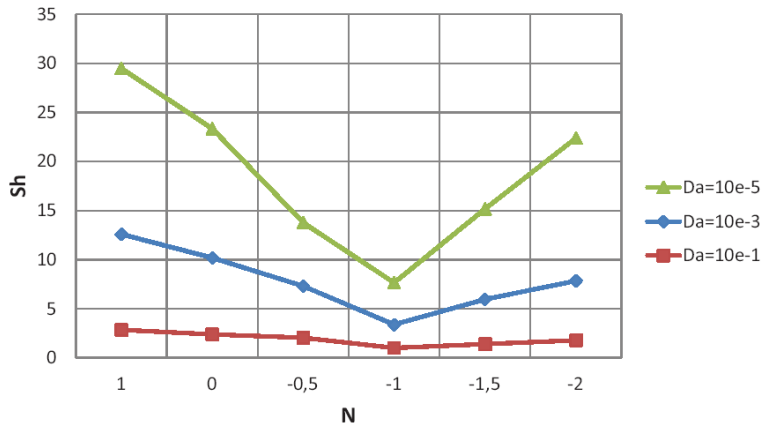

Figure 3: Sherwood number values for different Da and N.

in negative direction, e.g. $N < -1.5$, Nu and Sh values start to increase, in this case the mass and heat are transferred due to dominant solutal buoyancy force.

The onset of double-diffusive natural convection in the chosen geometry induces the main vortex in the $x - z$ plane, which is the reason the plane $y = 0.5$ is chosen to study temperature, concentration and velocity profiles. In Figs 4 and 5 the temperature and concentration profiles for $Ra_P = 100$, $Le = 10$, $Da = 10^{-3}$ and different values of buoyancy coefficient are presented. The highest temperature and concentration gradients can be observed near to the hot and the cold walls. In case, when $N = -1.5$ and $N = -2$, the profiles are close to the linear profile, the governing heat and mass transfer mechanism in this case is conduction. This phenomenon can be clearly seen from the Fig. 6 and 7, where the temperature and concentration fields are depicted. With decrease of N the isotherms and

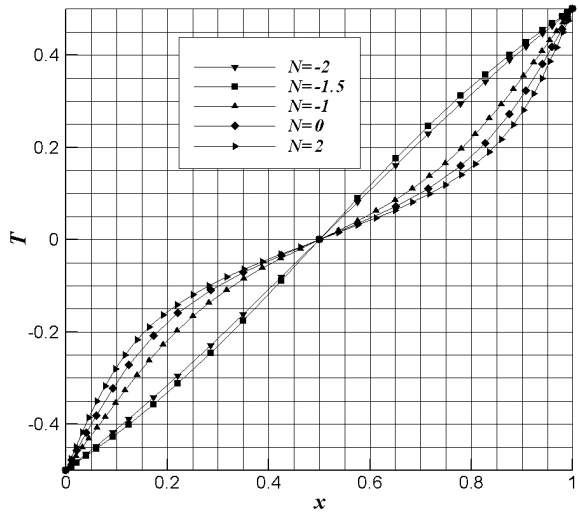

Figure 4: Temperature profiles at $y = 0.5$ and $z = 0.5$ for $Ra_P = 100$, $Da = 10^{-3}$, $Le = 10$ and various N.

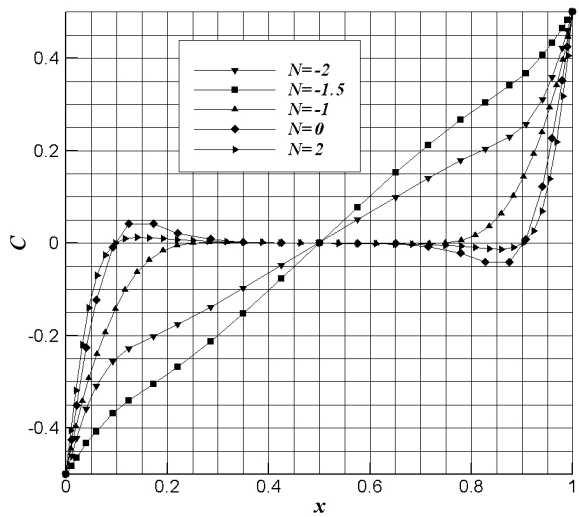

Figure 5: Concentration profiles at $y = 0.5$ and $z = 0.5$ for $Ra_P = 100$, $Da = 10^{-3}$, $Le = 10$ and various N.

iso-concentration lines become straight which clearly shows that the convective motion is diminished.

In addition, the streamlines for fix values of $Ra_P = 100$, $Le = 10$, $Da = 10^{-3}$ and different values of buoyancy coefficient are depicted in Fig. 8. It is obvious that

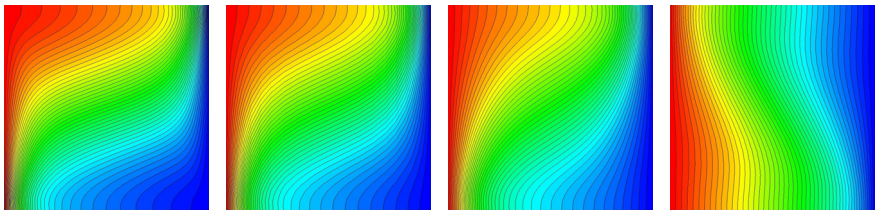

Figure 6: Temperature contour plots on the $Y = 0.5$ plane for $Ra_P = 100$, $Da = 10^{-3}$, $Le = 10$ and $N = 2$ (left), $N = 0$ (middle left), $N = -1$ (middle right) and $N = -2$ (right).

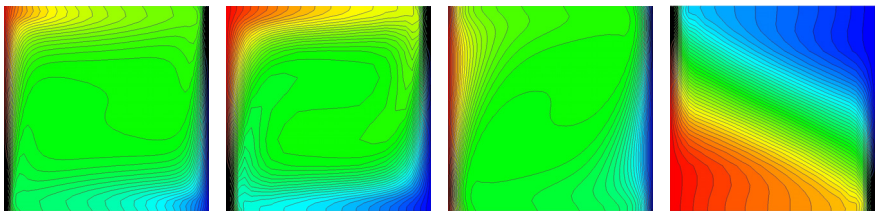

Figure 7: Concentration contour plots on the $Y = 0.5$ plane for $Ra_P = 100$, $Da = 10^{-3}$, $Le = 10$ and $N = 2$ (left), $N = 0$ (middle left), $N = -1$ (middle right) and $N = -2$ (right).

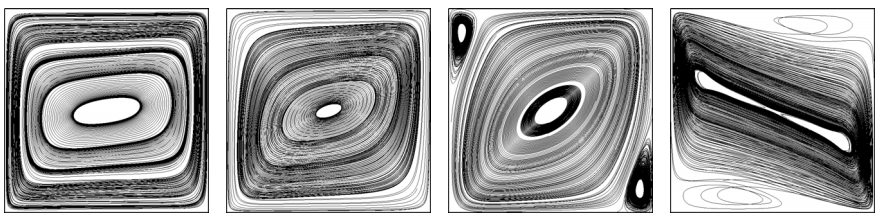

Figure 8: Streamlines on the $Y = 0.5$ plane for $Ra_P = 100$, $Da = 10^{-3}$, $Le = 10$ and $N = 2$ (left), $N = 0$ (middle left), $N = -1$ (middle right) and $N = -2$ (right).

the fluid is moving faster along the hot and cold walls, where the streamlines are closely spaced and the velocity gradient is high. With decrease of N from $N < -1$ the flow direction starts to turn in other direction and between $-1 > N > -1.5$ the velocity maximum starts to increase, the thickness of corresponding boundary layer again starts to decrease. It can be clearly observed from the flow field in Fig. 8 that the flow direction is reversed due to downward species buoyancy which dominates the flow as N becomes negative. Larger absolute values of buoyancy ratio result in stronger convective motion which enhances heat and mass transfer in the cavity.

From Fig. 9 where the iso-surfaces of absolute value of y velocity component are plotted can be clearly observed that the 3D nature of the phenomena occurs in the corners of the cubic cavity. Due to the fact that the flow field is driven by a large temperature and concentration difference between two opposite walls which causes 2D vortex in the y plane, the flow structure in the enclosure remains mainly two-dimensional. However, with increase of absolute values of N the movement perpendicular to the plane of the main vortex becomes more apparent.

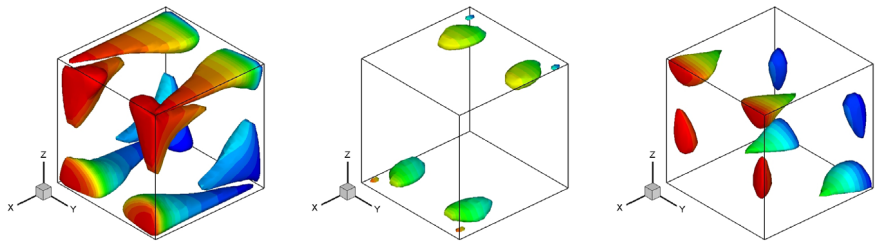

Figure 9: Isosurfaces for $Ra_P = 100$, $Da = 10^{-3}$, $Le = 10$ and $N = 2$ (left), $N = -1$ (middle) and $N = -2$ (right).

5 Conclusion

Three-dimensional study of combined heat and solute transfer in porous enclosure is investigated numerically using the algorithm based on the BEM. The velocity-vorticity formulation of governing set of equations was obtained which is based on the volume-averaged macroscopic Navier–Stokes equations. The numerical results for different values of governing parameters show good agreement to some available published results, which states the correctness of the obtained numerical scheme. Further study is focused on the influence of a limited number of dimensionless parameters, namely the Darcy number and buoyancy coefficient. The results state specific behavior of double-diffusive flow in porous media; the heat and mass transfer strongly depend on a Darcy number while the increase of the absolute value of buoyancy coefficient enhances the overall heat and mass transfer, in general. In the range when $0 > N > -2$, the thermal and solutal buoyancy effects start to oppose each other, which causes that the flow starts to flow in reversal direction. Three-dimensional nature of the flow becomes more apparent in cases when the absolute value of N is increasing, which is specially obvious in the corners of the cubic cavity.

References

[1] Murray, B.T. & Chen, C.F., Double-diffusive convection in a porous medium. *J Fluid Mech*, **201**, pp. 147–166, 1989.

[2] Trevisan, O.V. & Bejan, A., Combined heat and mass transfer by natural convection in a porous medium. *Advances in heat transfer*, **20**, pp. 315–348, 1990.
[3] Mahidjiba, A., Mamou, M. & Vasseur, P., Onset of double-diffusive convection in a rectangular porous cavity subject to mixed boundary conditions. *Int J Heat Mass Transfer*, **43**, pp. 1505–1522, 2000.
[4] Trevisan, O.V. & Bejan, A., Natural convection with combined heat and mass transfer buoyancy effects in a porous medium. *Int J Heat Mass Transfer*, **28**, pp. 1597–1611, 1985.
[5] Trevisan, O.V. & Bejan, A., Mass and heat transfer by natural convection in a vertical slot filled with porous medium. *Int J Heat and Mass Transfer*, **29**, pp. 403–415, 1986.
[6] Alavyoon, F., On natural convection in vertical porous enclosures due to prescribed fluxes of heat and mass at the vertical boundaries. *Int J Heat and Mass Transfer*, **36**, pp. 2479–2498, 1993.
[7] Goyeau, B., Songbe., J.P. & Gobin, D., Numerical study of double-diffusive natural convection in a porous cavity using the darcy-brinkman formulation. *Int J Heat Mass Transfer*, **39**, pp. 1363–1378, 1996.
[8] Sezai, I. & Mohamad, A.A., Three-dimensional double-diffusive convection in a porous cubic enclosure due to opposing gradients of temperature and concentration. *J Fluid Mech*, **400**, pp. 333–353, 1999.
[9] Mohamad, A.A., Bennacer, R. & Azaiez, J., Double diffusion natural convection in a rectangular enclosure filled with binary fluid saturated porous media: The effect of lateral aspect ratio. *Physics of fluids*, **16**, pp. 184–199, 2004.
[10] Bear, J., *Dynamics of Fluids in Porous Media*. Dover Publications, Inc., Mew York, 1972.
[11] Nield, D.A. & Bejan, A., *Convection in porous media (Third edition)*. Springer, 2006.
[12] Kramer, J., Ravnik, J., Jecl, R. & Škerget, L., Simulation of 3d flow in porous media by boundary element method. *Engineering Analysis with Boundary Elements*, **35**, pp. 1256–1264, 2011.
[13] Ravnik, J., Škerget, L. & Žunič, Z., Velocity-vorticity formulation for 3D natural convection in an inclined enclosure by BEM. *Int J Heat Mass Transfer*, **51**, pp. 4517–4527, 2008.
[14] Ravnik, J., Škerget, L. & Žunič, Z., Combined single domain and subdomain BEM for 3D laminar viscous flow. *Eng Anal Bound Elem*, **33**, pp. 420–424, 2009.